Compressive study on recycled concrete: experiment and numerical homogenization modelling

Fellah Djamel
University of Tizi ouzou, Algeria
Fellahdjamel92@gmail.com

Barboura Salma, Tilmatine Thileli
University of Sorbonne Paris North, France
salma.barboura@lspm.cnrs.fr, tilmatinethileli@gmail.com

Benyahi Karim, Kachi Mohand Said
University of Tizi ouzou, Algeria
karim.benyahi@ummto.dz, https://orcid.org/0000-0003-2033-6217
kachi_ms@yahoo.fr

Li Jia, Bouafia Youcef
University of Sorbonne Paris North, France
University of Tizi ouzou, Algeria
jia.li@univ-paris13.fr, youcef.bouafia2012@yahoo.com

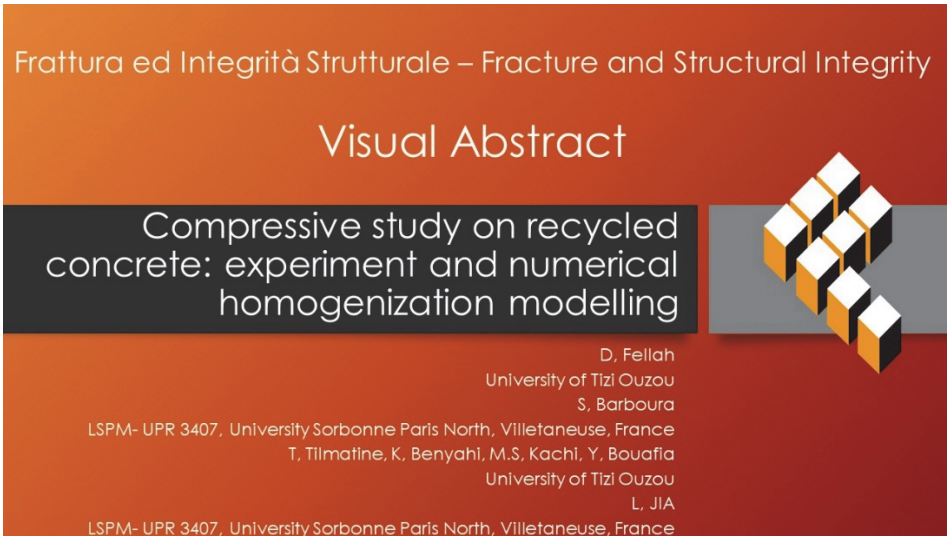

Citation: Fellah D., Barboura S., Tilmatine T., Benyahi K ., Kachi MS., Li J., Bouafia Y., Compressive study on recycled concrete: experiment and numerical homogenization modelling, Frattura ed Integrità Strutturale, 67 (2024) 58-79.

Received: 17.08.2023
Accepted: 22.10.2023
Online first: 28.10.2023
Published: 01.01.2024

KEYWORDS. Recycled concrete, Secant homogenization, Nonlinear modelling, Damage parameter.

INTRODUCTION

Recycled concrete (RC) made with recycled aggregates from crushing demolition waste offers economic, social, and environmental benefits compared to conventional concrete made with natural aggregates[1,2]. Generally, RC exhibits weaker mechanical properties than conventional concrete due to the properties of the recycled aggregates [3,4]. The compressive strength of recycled concrete (RC) is related to the properties and rate of recycled aggregates (RA). According to [3,5,6] , recycled aggregates cause a decrease in the compressive strength of recycled concrete. The mechanical properties and performance of such recycled aggregates are at least equal to the properties of natural concrete, which are in any case weaker than those of natural aggregates (NA). The decrease in mechanical properties of RC is also attributed to changes in the interfacial transition zone (ITZ) between aggregate and mortar resulting from the substitution of natural aggregates with recycled aggregates [7]. Experimental investigations have shown that the thickness of ITZ in RC is around 55 μm, leading to a decrease in the average modulus of ITZs by approximately 10-30 % compared to the matrix mortar surrounding the aggregates [8].

It is essential to examine the mechanical properties of recycled aggregates, old mortar, the interfacial phase between aggregates and old mortar, and the interfacial phase between old mortar and new mortar. These factors significantly influence the mechanical properties of RC. To understand the compressive behavior of RC as a fundamental characterization, various theoretical and numerical models have been developed, including empirical models, fracture mechanics approaches, and continuum damage mechanics[7,9] . These macroscopic models cannot clarify the link between the overall multiscale behavior of RC and its heterogeneities related to its constituent phases such as RA, NA, and pores. Therefore, advanced models based on homogenization theories, such as homogenization using the finite element method, have been proposed [10,11]. These models consider the behavior of individual phases and their interactions and can yield valuable insights into the mechanical behavior of recycled concrete. However, it is worth noting that these finite element calculations can be computationally intensive and time consuming. Recent research has introduced a combined finite element method and analytical multiscale model that evaluate the effective elastic properties of recycled concrete using a MoriTanaka homogenization technique [11]. This model captures the behavior of the material at different scales, limited to only the elastic domain. The developed multiscale modeling demonstrates good agreement with experimental results in elasticity. Another micromechanic analytical model predicts the strength of recycled concrete by considering the microstructure at different scales and incorporating a Drucker-Prager criterion for hydrate failure mechanisms at the microscopic scale [12]. In this work, the study concerns the sensitivity of several parameters, such as old mortar content, water/cement ratio, and aggregate replacement ratio, but the behavior and evolution of the mechanical properties under loading have not been discussed. Recently, Gupta et al. [11]developed an analytical multiscale model based on a coated inclusion to predict the concrete's behavior. The considered microstructure of the whole concrete is constituted by multi-coated aggregate embedded in the cement paste [13]. These coated layers, or interfacial transition zones (ITZ), considered at the scale of cement paste as a composite formed with fine inclusions (clinker phase, hydration products, pores) embedded in C-S–H gel forms are numerically specified using the cement hydrate platform [14] to deduce the thickness of the ITZ and homogenized using the Mori-Tanaka model. The damage in each ITZ layer and cement paste is modeled based on a threshold strain value of cement paste, which results in a reduction of the elastic modulus of concrete and leads to nonlinear stress-strain behavior. The approach of Gupta et al. predicts the behavior of concrete up to peak stress but does not study the post-peak phase of the stress-strain curve. In addition, obtaining accurate mechanical properties at the lowest scale may be challenging and lead to additional difficulties.

Based on experimental compressive study, in this work we aim to develop a numerical homogenization modelling using multiphase mean field model in a general consideration as the form of aggregate to catch the complex behavior of the recycled concrete beyond elastic state. We propose on the basis of continuum micromechanics a simple analytical method able to consider the ITZ in the concrete to predict stress strain compression behavior of several recycled concretes. Initially, the homogenization development concerns the elastic stage of recycled concrete [15,16]. The model has demonstrated its potential in predicting the elastic properties of several recycled concretes, drawing inspiration from the work of Cammacho [17] and Pierard [18]. Using the secant linearization, the prediction of the nonlinear behavior of composite can be established from the behavior of their individual constituents and the secant properties of each phase can be evaluated at each loading step according their local behavior law. At each step, the linear homogenization model can be applied. The main advantage of the secant homogenization methods is (i) the good qualitative agreement between their predictions and the results obtained by finite element method, and (ii) the suitable description of the composite response under monotone loading [19,20] . The approach presented in this work, combined with planned experimental investigations, can be highly beneficial in predicting the mechanical behavior of recycled concrete structures. This integration of theoretical analysis with practical

experimentation is crucial for achieving a comprehensive understanding of the performance of such structures, ultimately contributing to their safe and sustainable design. The forthcoming experimental work will involve conducting a series of tests and measurements on recycled concrete specimens. These experiments will encompass various mechanical properties, including Young moduli, compressive strength and workability. By subjecting the specimens to the compressive loading and carefully monitoring their response, valuable data will be gathered to assess their structural behavior and performance. The results obtained from these experiments will provide critical insights into the mechanical characteristics of recycled concrete, aiding in the prediction of its performance in real-world applications. Several aspects of RC have been investigated in previous studies within the literature. These include examining the stress-strain relationship, determining compressive strength, analyzing the effects of uniaxial compression, studying different strengths of parent concrete [5,6], measuring water absorption capacity [19], exploring various types of coarse aggregates [16] , investigating different mix designs and mixing methods, and assessing the levels of recycled aggregate replacement. A multiscale numerical model is also developed and applied to analyse the creep of the recycled concrete [16].
This paper is organized as follows: the first part is devoted to the experimental campaign at the macroscopic scale (method, material, tests, and results). Whereas the second part presents the modeling of the linear elastic behavior of RC and the proposed extension to simulate uniaxial loading. The numerical algorithm is also exposed in a third section. In Section 4, several applications are proposed. Firstly, the effective Young modulus is compared to experimental measures. Secondly, the simulations of the uniaxial compressive loading are confronted with the test results of RC with 25, 50, and 75 % of RA. The proposed model is finally used to simulate other RCs from the literature. In the end, some concluding remarks and perspectives are stated.

Experimental study

The experimental program takes into account the volume ratio at which recycled aggregates are replacing natural aggregates. Four types of concrete samples are prepared. The first one is a natural concrete NC prepared only with natural aggregates; the other three types of samples are recycled concrete RC, in which the natural aggregates NA are substituted by recycled aggregates RA with different substitution rates (25%, 50%, and 75%), in order to study and analyse the influence of recycled aggregates on the properties of the concrete.

Materials

The cement used in this study is produced by a local company of the CPJ-CEM II/B 42.5 N type, with a characteristic hardened strength of 42.5 MPa and also complying with the Algerian (AN) and European (EN 197-1) standards. Its fineness modulus, according to the Blaine method, is 3700-5200 g/cm2. The natural aggregates NA are provided by a quarry and are produced after crushing rocks from quarries. They are divided into three granular classes: sand (0/3mm), gravel (3/8 mm), and gravel (8/15mm). The recycled aggregates RA are obtained after crushing and grinding demolition waste. The production of the recycled aggregates is done at the level of a local quarry. Recycled aggregates are divided into two classes: gravel (3/8mm) and gravel (8/15mm). The recycled aggregate is made up of two phases: an old mortar with a fraction of 0.6 and an original aggregate with a fraction of 0.4.

Figure 1: Waste used to obtain recycled aggregates (right): demolition waste from laboratory waste (left).

Sieve analysis was first performed in order to determine the distribution by weight of the particles of a material according to their dimensions (NF P 18-560).

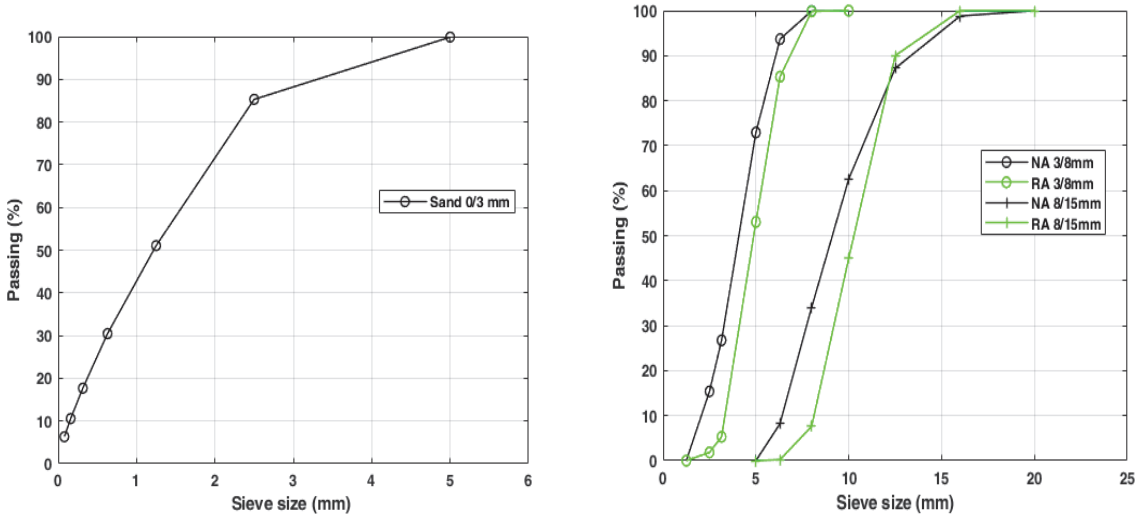

a)- Sieve analysis of natural sand 0/3 mm. b)- Sieve analysis of the NA and RA.

Figure 2: sieve analysis of used materials.

Fig. 2.a shows the sieve analysis of the sand (0/3mm) while Fig. 3.b shows the sieve analysis of the NA and the RA of fractions (3/8mm) and (8/15mm) respectively. We notice a slight difference in percentage of sieve between the NA and the RA [17]. Some physical properties of the used NA and RA are shown in Tab. 1.

Material	Sand 0/3 mm	NA 3/8 mm	NA 8/15 mm	RA 3/8 mm	RA 8/15 mm
Bulk density (kg/m³)	1680	1486	1481	1212	1258
Absolute density (kg/m³)	2670	2565	2565	2521	2521
Absorption (%)	2.87	1.42	0.89	5.5	4.95
Lac (%)	/	30.49	33.24	30.1	34.74
Fineness modulus	3.05	/	/	/	/

Table 1: Properties of the used aggregates (sand, NA and RA).

According to Tab. 1, the bulk and absolute density of the RA are lower than those of the NA, the absorption of NA (3/8mm) and NA (8/15mm) is 1.42% and 0.89%, and the absorption of RA (3/8mm) and RA (8/15mm) is 5.5% and 4.95% [21]. It can be seen that the absorption of RA is five times that of NA. The decrease in weight and the increase in absorption of RA are directly attributed to the old mortar attached around the original aggregate. The old mortar contains voids and pores that, on the one hand, reduce the weight and, on the other hand, increase the absorption capacity. The Los Angeles coefficient (Lac) of RA (8/15 mm) is higher than that of NA (8/15mm) by 4.4%, which is attributed to the low wear resistance of the old mortar attached to the recycled aggregates [20]. On the other hand, the Lacs of NA (3/8mm) and RA (3/8mm) are slightly different. Therefore, their fragmentation resistance is almost the same. The water used is the water available at the laboratory level, which is potable tap water.

Concrete specimens

The Dreux-Gorisse method is used for the formulation of concrete [22]. The objective of this method is to determine, according to workability and resistance, the nature and quantity of materials necessary for the construction of one cubic meter of concrete (water, cement, sand, and gravel in kg/m³). The prepared concrete is plastic concrete, which has a resistance of 25 MPa at the age of 28 days. In order to have clean materials devoid of all impurities, the aggregates are washed and then dried in a drying room for 24 hours at a temperature of 105 °C. In this work, four types of samples of

concrete were realized, noted as NC, RC25, RC50, and RC75, respectively, in which 0%, 25%, 50%, and 75% of NC were replaced by RA. The formulation of the different types of samples is shown in Tab. 2.

Figure 3: Materials used in the manufacture of concrete.

Material in (kg)	NC	RC25	RC50	RC75
Cement	400	400	400	400
Water	228	228	228	228
sand (0/3)	616.77	616.77	616.77	616.77
Natural aggregate (3/8)	169.29	126.9675	84.645	84.645
Recycled aggregate (3/8)	0	41.5965	83.193	83.193
Natural aggregate(8/15)	1049.6	787.19	524.799	262.4
Recycled aggregate(8/15)	0	249.8166	499.6332	749.45

Table 2: Formulation of Samples NC, RC25, RC50 and RC75.

For each type of concrete, three cylindrical samples (diameter 16cm and height 32cm) are prepared to determine the properties of the concrete in its hardened state. All these samples are cast in steel molds and prepared under the same conditions. We start with the preparation of materials (water, cement, sand, and gravel), then moisten the walls of the mixer. The materials are put into the mixer successively, from the largest diameters to the smallest. After the materials are kneaded in a dry state for 30 seconds, add 10% mixing water and mix for 30 seconds. Finally, the rest of the mixing water is added and mixed for one minute and 30 seconds. The molds filled with concrete are vibrated using a vibrating table. The concrete specimens are kept for one day in molds in the laboratory at 25°C, removed 24 hours after casting, and kept in water until the day of testing, i.e. at the age of 28 days.

Experimental tests

Slump test. The slump test is used to determine the consistency of concrete by measuring its slump value under its own weight. This test is carried out on the different concrete formulations (NC, RC25, RC50 and RC75). The slump test results allow us to evaluate the effect of RA on fresh concrete parameters as well as its rheological properties. Ultrasonic pulse velocity (UPV) test. This test is used to determine the quality of the material, by measuring the speed of an ultrasonic wave passing through the tested element. This velocity is high when the material is compact and resistant, and vice versa. A piezoceramic source is electrically pulsed to generate ultrasonic waves that travel in the structural element and are then

sensed by the receiver on the opposite side of the sample. The source and receiver signals are recorded by an Olson Instruments data collection platform equipped with an UPV system.

a) The Abrams cone slump test. b) Ultrasonic pulse velocity (UPV) test. c) Compression test device.

Figure 4: Experimental testes realised in laboratory.

Compression test. This test aims to determine the maximum compressive strength and the initial Young's modulus of the concrete samples at the age of 28 days. The compression test is carried out using an hydraulic press of load capacity of 2000 kN, the concrete specimen is subjected to a progressive loading, with a step of loading of 0.5 kN/second, the load applied is displayed on the machine screen and the shortening of the concrete is given by comparators, for each step of loading, one records the force and the corresponding deformation. The experimental device does not make it possible to follow the evolution of the curve of behaviour after the peak of deformation, because the reading of the deformation on the comparators in the phase after peak becomes difficult.

Results and discussion

According to the results presented in Tab. 3, the NC prepared only with NA has a slump of 8.5cm and the RC25 has a slump of 7.5cm, then both are plastic concrete, the RC50 has a slump of 5mm and the RC75 has a slump of 2.5mm, then both are firm concrete. From these results, it can be seen that the NC and the RC25 have the same consistency, so a substitution of 25% of NA by RA does not affect the condition of fresh concrete [23] . However, the further increase in RA leads to a significant decrease in slump and a change in consistency [24]. These remarks are attributed to the addition of recycled aggregates (RA), which have a high absorption due to the voids present in the old mortar adhered to the original aggregate, and therefore, a higher rate of RA will increase the porosity, which absorbs more water from the mixing, leading to a decrease in slump and changing the consistency of the concrete [25]. The results of the ultrasonic pulse velocity tests are also shown in Tab. 3. The NC shows better quality than the other concretes. As indicated in some previous investigations [26], the speed of the ultrasonic waves decreases with the increase of the RA ratio. The increase in the RA ratio leads to increased porosity in recycled concrete, which affects the transmission of ultrasound waves in concrete and causes a velocity slowdown[27].

Type	Slump(cm)	UPV (m/s)	Compressive strength (MPa)	Elastic modulus (MPa)
NC	8.5	4893	27.13	25868
RC25	7.5	4830	26.43	23678
RC50	5	4725	25.65	21937
RC75	2.5	4687	24.84	20210

Table 3: Experimental results.

From Tab. 3, we can observe that the compressive strength of the samples decreases as the RA ratio increases from 2.6% for RC25 to 8.44% for RC75 compared with the NC. This decrease in strength is directly attributed to the mechanical and physical properties of recycled aggregate RA[28], as these are of lower quality than those of natural aggregate NA [29].

Fig. 5 shows the stress-strain curve of all samples recorded in the uniaxial compression test. According to this figure, the behavior curves can be divided into three parts. The first part is presented by the linear zone; the second is the nonlinear zone of the ascending branch; and the third part is represented by the descending branch [30] . We can notice that the concrete behavior curve changes with the incorporation of RA [31], from which we see an influence of RA on the concrete behavior. It is clear that the increase in the RA ratio induces a reduction of the initial elastic modulus as well as a reduction of the peak stress [3]. The increase in the RA ratio increases the peak strain as well as the curvature flattening in the post-peak phase. In fact, when the NA is replaced by the RA, the presence of interphase ITZ's such as new mortar-natural aggregate, old mortar-original aggregate, and old mortar-new mortar induces more easily the development of microcracks and therefore reduces the concrete resistance as well as the elastic modulus [31].

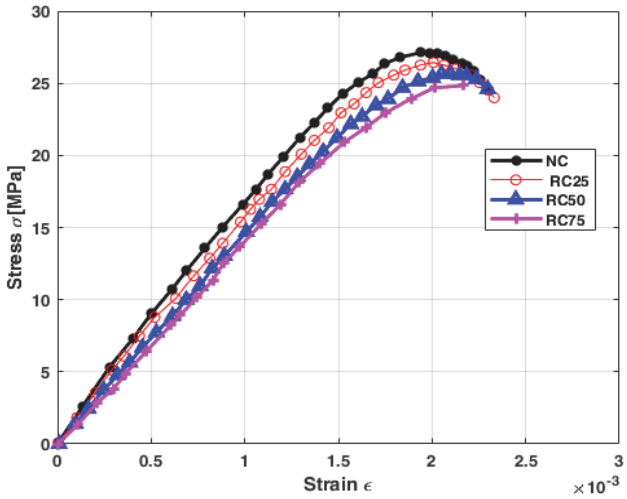

Figure 5: Behavior in uniaxial compression of concrete NC, RC25, RC50 and RC75.

The Young modulus depends on the phases that constitute the concrete. According to Tab. 3, the Young moduli of recycled concrete (RC25, RC50, and RC75) are lower than those of NC. The decrease in Young's modulus is a function of the replacement rate [32]. This decrease is attributed to recycled aggregates (RA), which have lower elastic rigidity compared to natural aggregates (NA).

NUMERICAL MODELLING OF RECYCLED CONCRETE MATERIALS

In the subsequent sections, we present a simplest and efficient numerical model based on the multiphase homogenization method. This model enables the prediction of the behavior of recycled concrete RC, encompassing both linear and nonlinear domains. In a previous work [33], the representative volume element RVE of recycled concrete is presented by three phases, new mortar NM, aggregates (recycled and natural aggregates) and voids. In the concrete microstructure, it is important to take into account the thin layers between aggregates and mortar that can include modified elastic properties from mortar called in several work as interfacial transition zone (ITZ). The mechanical identification properties of these interfacial zone required high performance experimental equipment like nanoindentation, Atomic Force Microscopy (AFM), Scanning Electron Microscopy (SEM), and specific procedures for grinding and polishing specimens [8,34]. From Xiao et al experimental investigations [8] , the thicknesses of ITZ in recycled aggregate (between old mortar and NA) and in recycled concrete (between new mortar and aggregates) are found to be around 55µm which is very small volume fraction compared to aggregates in concrete. Moreover, the average modulus of ITZs appears to be approximately 70-90% of that of matrix mortar modulus surrounding the aggregates.

Nonlinear homogenization processing

The basic methodology for dealing with the non-linear behavior of heterogeneous materials on the basis of its representative volume element (RVE), in particular the RVE of recycled concrete, requires a set of simplifying assumptions to solve this complex problem. To do so, it is required to substitute the non-linear problem with a series of successive linear problems. It is important (i) to examine and clarify the behavior of each phase of recycled concrete when loads are applied and (ii) to

understand the link between the local strain and stress fields and the macroscopic loading imposed to the representative volume element of the recycled concrete.
In the nonlinear framework, the mechanical properties of each constitutive phase of the recycled concrete depend on the strain-stress loading history. To process nonlinear homogenization, a linearization method has to be applied at each loading level. This linearization enables the use of a suitable linear homogenization method designed specifically for recycled concrete [33].
Recently, in Barboura's work [35], the secant linearization is used to assess the elastoplastic of co-continuous composite. This secant linearization preserves the overall symmetry of the phases and the composite material throughout the monotonic loading. It establishes a linear relationship between the mean stress and strain of each phase as on can see the Fig. 6 [36]. It provides a straightforward and intuitive way to characterize the mechanical response of each phase which the constitutive behavior can be described as follows:

$$\boldsymbol{\sigma}^{(I)}(\mathrm{y}) = \mathbf{C}_{sct}^{(I)}(\boldsymbol{\varepsilon}^{(I)}(\mathrm{y})) : \boldsymbol{\varepsilon}^{(I)}(\mathrm{y}) \tag{1}$$

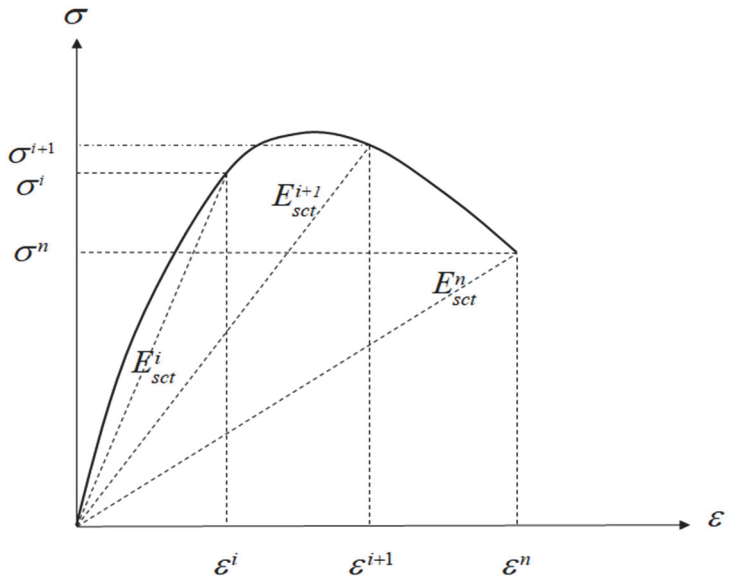

Figure 6: Secant linearization.

The secant stiffness tensor depends on the mean local strain field of each phase (I=NM, NA and RA) in the two-phase domain G_i can be rewritten as follows:

$$\boldsymbol{\sigma}^{(I)}(\mathrm{y}) = \mathbf{C}_{sct}^{(I)}(\langle\boldsymbol{\varepsilon}(\mathrm{y})\rangle_I) : \boldsymbol{\varepsilon}^{(I)}(\mathrm{y}) \tag{2}$$

Then the effective grains Gi can be estimated by:

$$\langle\boldsymbol{\sigma}(\mathrm{y})\rangle_{G_i} = \mathbf{C}_{\mathrm{sct}_{G_i}}^{\mathrm{hom}}(\mathbf{E})\mathbf{E} \tag{3}$$

where $C_{\mathrm{sct}_{G_i}}^{\mathrm{hom}}$ is the effective stiffness tensor of grain (G_i). The relationship between $\langle\boldsymbol{\varepsilon}(\mathrm{y})\rangle_I$ and $\mathbf{E}$ is given by the localization tensor of the mean secant strain of order 4 of phase (I) as follows:

$$\langle\boldsymbol{\varepsilon}(\mathrm{y})\rangle_I = \mathbf{A}_{\mathrm{sct}}^{I}\left(\mathbf{C}_{\mathrm{sct}_{G_i}}^{\mathrm{hom}}, \mathbf{C}_{\mathrm{sct}}^{I}, f_{NM}, \langle\boldsymbol{\varepsilon}(\mathrm{y})\rangle_I\right)\mathbf{E} \tag{4}$$

(Eq.4) presents a nonlinear problem, because the average strain in each phase $\langle\boldsymbol{\varepsilon}(\mathrm{y})\rangle_I$ depends on the localization tensor $\mathbf{A}_{\mathrm{sct}}^{I}$, the localization tensor itself depends on the average strain in the phase.

$$\mathbf{A}_{sct}^{NM} = \frac{1}{\left(1 - f_{inc}\right)}\left(\mathbf{C}_{sct}^{NM} - \mathbf{C}_{sct}^{inc}\right)\left(\mathbf{C}_{sct_{G_i}}^{hom} - \mathbf{C}_{sct}^{inc}\right), \left(inc = NA, RA, voids\right) \quad (5)$$

$$\mathbf{A}_{sct}^{inc} = \frac{1}{f_{inc}}\left(\mathbf{C}_{sct}^{inc} - \mathbf{C}_{sct}^{NM}\right)\left(\mathbf{C}_{sct_{G_i}}^{hom} - \mathbf{C}_{sct}^{NM}\right), \left(inc = NA, RA, voids\right) \quad (6)$$

The secant mean phase localization tensor depends on the linearized phase properties at the current loading step and the linear homogenization method of the heterogeneous material described below.

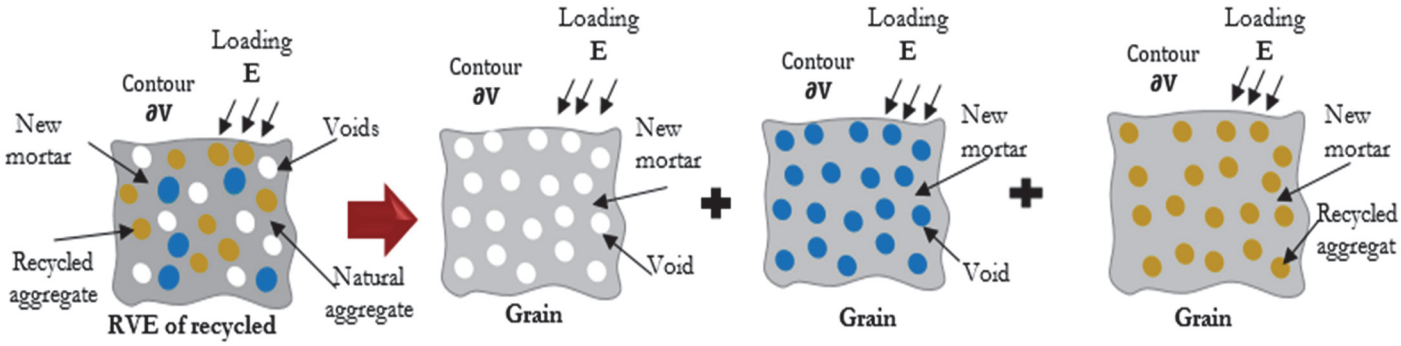

Figure 7: Grains subjected to a macroscopic deformation E.

Elastic homogenization method for recycled concrete

The coupling of secant linearization with the three-step homogenization method [33] makes it possible to describe the behavior of multi-phase composites. First, the behavior of each phase of the composite is linearized by a secant approach, and then the behavior of the multi-phase composite is determined by the three-step homogenization method. In this part, we propose to extend the elastic homogenization model [33] to predict the nonlinear behavior of RC. This model is based on the secant linearization procedure of the nonlinear behavior of the constitutive phases. The imposed macroscopic strain field **E** on the RVE is assumed to be the same for each decomposed grain, which is equal to the average of the local strains in the recycled concrete RVE (see Fig.7):

$$\langle \boldsymbol{\varepsilon} \rangle_{RVE} = \mathbf{E} \quad (7)$$

The symbols < . > indicate the average over the volume of the RVE.

$$\langle . \rangle = \frac{1}{V}\int_{V} . dV \quad (8)$$

In a nonlinear case, the properties of each phase of grains G_i become dependent on the macroscopic loading E applied to their contour. The secant linearization method consists of replacing any nonlinear behavior by a sequence of linearized behavior phases. This secant approximation method links the stress field of each phase of grains G_i to the local deformation field by the secant stiffness tensor C_{sct}. In general, this constitutive behavior can be described using deformation theory as follows:

$$\boldsymbol{\sigma}(y) = \mathbf{C}_{sct}(\boldsymbol{\varepsilon}(y)) : \boldsymbol{\varepsilon}(y) \quad (9)$$

As previously described, the representative volume element (RVE) of RC can be viewed as a multiphase composite constituted by a matrix (new mortar), and inclusions, namely RA, NA, and voids. The form and properties of the inclusions can be different and are randomly distributed. To obtain the effective properties of RC, we adapt a multiphase homogenization procedure as described in [18]. This elastic homogenization is based on a multistage homogenization

method depending on the complexity of the microstructure. In this study, we propose a homogenization strategy composed of three homogenization steps.

First step

In the first step, we determine the effective properties of the recycled aggregate (RA), by using a homogenization model recently developed in [37] named GEEE model, serves as a powerful estimator for calculating the equivalent stiffness of multiphase ellipsoidal heterogeneities. The estimator is formulated explicitly, which facilitates its implementation in a computational program. The recycled aggregate is composed of two phases, old mortar (OM) with a stiffness tensor of $\mathbf{C}_{OM}$ and original aggregate (OA) with a stiffness tensor of $\mathbf{C}_{OA}$.

At this stage, we can determine an equivalent stiffness tensor $\mathbf{C}_{eq}^{RA}$ of the recycled aggregate (RAeq), which can be explicitly expressed as follows:

$$\mathbf{C}_{eq}^{RA} = \mathbf{C}^{OM} + f_{OA}\left[\left(\mathbf{C}^{OA} - \mathbf{C}^{OM}\right)^{-1} + \left(\mathbf{P}^{OA} - f_{OA}\ \mathbf{P}^{eq}\right)\right]^{-1} \tag{10}$$

with:

$$\mathbf{P}^{OA} = \mathbf{S}^{OA} : \left(\mathbf{C}^{OM}\right)^{-1} \text{ and } \mathbf{P}^{eq} = \mathbf{S}^{eq} : \left(\mathbf{C}^{OM}\right)^{-1} \tag{11}$$

$\mathbf{P}^{OA}$ denotes the Green operator related to Eshelby $\mathbf{S}^{OA}$ relative to the form of the original aggregate (OA) surrounded by old mortar matrix (OM). The presence of the interface transition zone (ITZ_{OA}^{OM}) in recycled aggregate or several coated interfaces ($ITZ_{OA}^{OM(n)}$) can be taken into account by the GEEE model using an iterative procedure, as explained in Gazavizadeh et al.'s work [37]. This interphase is located between the original aggregate (OA) and the old mortar (OM). In this case, to obtain an equivalent recycled aggregate, we use two iterations of the GEEE model. Similarly, by using the GEEE model, the interface (ITZ_{NA}^{NM}) between the natural aggregate NA and the new mortar can be taken into account, so the natural aggregate is considered an inclusion surrounded by a layer of new mortar. Thus, we obtain an equivalent natural aggregate NA_{eq}.

Second step

The RVE of recycled aggregate is decomposed into grains (G_i). Each grains is constitute by two phases, new mortar NM as a matrix and aggregates as inclusion (NA_{eq} or RA_{eq}), the volume fraction of NM in the VER is the same for all grains (G_i) The inclusions of the same form are distributed randomly in the matrix. To homogenize each grain on its local axis linked to the inclusion form, we can use the Mori Tanaka model and obtain:

$$\mathbf{C}_{G_i} = \mathbf{C}_{NM} + (1 - f_{NM})\left(\mathbf{C}_I - \mathbf{C}_{NM}\right) : \left[\mathbf{I} + f_{NM}\mathbf{P}^{NM} : \left(\mathbf{C}_I - \mathbf{C}_{NM}\right)\right]^{-1} \tag{12}$$

where $\mathbf{C}_{G_i}$ denotes the stiffness of grain, $\mathbf{C}_I$ denotes the stiffness of inclusion. In the case of porous phases, the homogenized tensor of grain can be expressed as follows:

$$\mathbf{C}_{G_i} = \mathbf{C}_{NM} + (1 - f_{NM})\mathbf{C}_{NM} : \left[\mathbf{I} - f_{NM}\mathbf{P}^{NM}\ \mathbf{C}_{NM}\right]^{-1} \tag{13}$$

with $\mathbf{I}$ denotes the identity tensor of order four and $\mathbf{P}^{NM}$ the Green operator related to Eshelby tensor $\mathbf{S}^{NM}$ relative to the form of the aggregate (RAeq or NA) or voids surrounded by new mortar matrix (NM) .

For a random distribution of inclusion in grains (G_i), we need to take into account the effect of the inclusion orientation in the matrix on the macroscopic properties. The random orientation distribution is represented by the Euler angles (θ, φ,

ψ). We simply require average over the all direction of orientation of the effective stiffness tensor of the two-phase grain (G_i)

$$\left(\mathbf{C}^{\hom}_{G_i}\right)_{ijkl} = \frac{1}{8\pi^2}\int_0^{2\pi}\int_0^{\pi}\int_0^{2\pi} a_{im}a_{jn}a_{kp}a_{lq}\left(\mathbf{C}_{G_i}\right)_{mnpq}\sin\theta d\theta d\phi d\psi \tag{14}$$

Where a_{ij} are the coefficients of the rotation matrix, allowing the transformation of a fourth-order tensor from one frame into another following the Euler angles.

Third step

The RVE of recycled concrete is made up of homogenized grains G_i, which constitutes a multi-phase composite, according to Pierrad [18], the macroscopic behaviour of recycled concrete can be determined by the Voigt model:

$$\mathbf{C}_{\hom} = \sum_{i=1}^{N} f_{Gi}\mathbf{C}^{\hom}_{G_i} \tag{15}$$

with f_{Gi} denotes the volume fraction of gain G_i, $f_{G_i} = \frac{f_I}{1 - f_{NM}}$ (I=NA, RA, voids).

Assumption for natural and recycled aggregates in the concrete

The real RA or NA can be assumed to be of spheroidal form and randomly distributed in the new mortar. A statistical measure of the minimum and maximum width of natural or recycled aggregate after sieve analysis shows that the aspect ratio is between 0.5 and 2. To justify the choice of spherical aggregates, we compare the effective properties of two concretes: the first contains spherical aggregates, and the second contains spheroidal aggregates. Both aggregates are randomly distributed in the new mortar. Fig.8 presents the normalized Young modulus with respect to aspect ratio, from oblate to prolate forms of inclusion for the two concretes. We observe that the values of the normalized Young modulus of concrete with randomly oriented spheroidal aggregates converge to those with spherical aggregates. We can note that when the aspect ratio is between [0.5 and 2], the difference is not significant, as shown in Fig.8. In the simulation, for the sake of simplicity, the form of aggregates is taken as spherical.

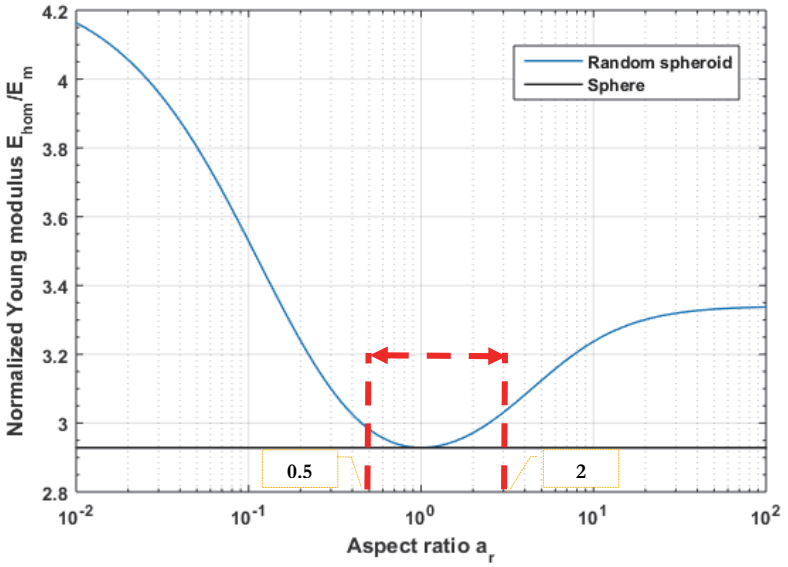

Figure 8: Normalized Young's modulus as a function of aspect ratio.

To resume, the homogenized stiffness tensor $\mathbf{C}_{\text{sct}_{G_i}}^{\text{hom}}$ relates the macroscopic strain load to the average stress of grain G_i. That is the key for the secant homogenization procedure to correctly estimate the constitutive behavior. The homogeneous secant stiffness tensor of each grain is determined by Mori Tanaka's two-phase homogenization scheme:

$$\mathbf{C}_{\text{hom}_{G_i}}^{\text{sct}} = \mathbf{C}_{\text{NM}}^{\text{sct}} + (1 - f_{\text{NM}})\left(\mathbf{C}_{\text{I}}^{\text{sct}} - \mathbf{C}_{\text{NM}}^{\text{sct}}\right) : \left[\mathbf{I} + f_{\text{NM}}\mathbf{S}_{\text{esh}}\left(\mathbf{C}_{\text{NM}}^{\text{sct}}\right)^{-1} : \left(\mathbf{C}_{\text{I}}^{\text{sct}} - \mathbf{C}_{\text{NM}}^{\text{sct}}\right)\right]^{-1} \tag{16}$$

The aggregate obtained is a multi-phase composite, which is homogenized with the Voigt model as follows:

$$\mathbf{C}_{\text{hom}}^{\text{sct}} = \sum_{i=1}^{N} f_{Gi}\mathbf{C}_{\text{hom}_{G_i}}^{\text{sct}} \tag{17}$$

$$\mathbf{\Sigma}_{\text{RC}} = \mathbf{C}_{\text{hom}}^{\text{sct}}(\mathbf{E})\mathbf{E} \tag{18}$$

Behaviour of the constituent phases of recycled concrete

In this section, we describe the essential behaviour laws that govern each phase of concrete, covering aggregates and mortar. These laws are crucial to understanding how concrete behaves under different loading conditions, including compression.

Aggregates

The natural aggregates NA and the equivalent recycled aggregates RAeq, represent the reinforcement or inclusion phases in the recycled concrete. The behaviour of the NA and RAeq is assumed to be linear elastic, so the average stress in those two phases is linearly linked to the average strain.

Matrix

The new mortar is governed by the Mazars [39,40] damaged law, widely used in the literature [41,42], the decrease of the material rigidity under effect of micro cracks is driven by a scalar internal variable D. The stress-strain relationship is given by the following equation:

$$\overline{\boldsymbol{\sigma}}^{(\text{NM})} = \mathbf{C}_{\text{sct}}^{(\text{NM})}\left(\overline{\boldsymbol{\varepsilon}}^{(\text{NM})}\right)\overline{\boldsymbol{\varepsilon}}^{(\text{NM})} = (1 - \text{D})\,\mathbf{C}^{(\text{NM})}\,\overline{\boldsymbol{\varepsilon}}^{(\text{NM})} \tag{19}$$

The variable of damage D results from a combination of a traction damage D_t and a compression damage D_c, it can be written as follow:

$$D = \alpha_t^{\beta} D_t + \left(1 - \alpha_t\right)^{\beta} D_c \tag{20}$$

The coefficient α_t which carries out the coupling between the damage in traction and the damage in compression, it is equal to 0 in the total absence of traction, and equal to 1 in the total absence of compression.
The damage decompositions under traction or compression are defined by the following equations:

$$D_c = 1 - \frac{\left(1 - A_c\right)}{\varepsilon_{eq}} - A_c \exp\left(-B_c\left(\varepsilon_{eq} - \varepsilon_D^0\right)\right) \tag{21}$$

$$D_t = 1 - \frac{\left(1 - A_t\right)}{\varepsilon_{eq}} - A_t \exp\left(-B_t\left(\varepsilon_{eq} - \varepsilon_D^0\right)\right) \tag{22}$$

ε_D^0 : The threshold strain of damage.

β, A_t, A_c, B_t and B_c : Material parameters to identify.

ε_{eq} : The equivalent strain which controls the damage D in the material and defines the load surface f , such that:

$$f = \varepsilon_{eq} - K(D) = 0 \tag{23}$$

with: $K(D) = \varepsilon_{eq}$ if $D = 0$

As extension is the main reason of the concrete cracking, the equivalent strain is defined as follows:

$$\varepsilon_{eq} = \sqrt{<\varepsilon_1>_+ + <\varepsilon_2>_+ + <\varepsilon_3>_+} \tag{24}$$

where $<\varepsilon>_+$ is the positive part of the principal strains defined as follows:

$$<\varepsilon_i>_+ = \varepsilon_i \quad \text{if} \quad \varepsilon_i > 0 \tag{25}$$

$$<\varepsilon_i>_+ = 0 \quad \text{if} \quad \varepsilon_i < 0 \tag{26}$$

General algorithm

We apply the secant homogenization strategy to multiphase concrete composites by taking the behavior law of each constituent into account. The new mortar matrix (NM) is governed by the Mazars [39,40] damage law. The two types of inclusions, NA and RAeq remain linear and elastic. In the secant formulation, the macroscopic stress and the stiffness tensor $\mathbf{C}_{hom}^{sct}$ are calculated at each step of macroscopic loading. In the following, in order to simplify the notation, the domain of a pseudo-grain (G_i) is denoted by (V), its constituents are denoted by (V_{NM}) for the mortar matrix, and (V_I) for the inclusion phase (NA) or (RAeq).

The numerical algorithm starts with the knowledge of the applied macroscopic strain $\mathbf{E}_{n+1} = \mathbf{E}_n + \Delta\mathbf{E}$ at step (n+1). The properties of each phase of the recycled concrete (NM, NA, and RA_{eq}) are known in the previous step (n).

- Loop on each pseudo grain G_i
- Initialization in the new mortar matrix phase $<\boldsymbol{\varepsilon}>_{NM} = \mathbf{E}$.
- Call the Mazars model with $<\boldsymbol{\varepsilon}>_{NM}$ as an argument, this model gives us the secant stiffness of the matrix $\mathbf{C}_{NM}^{sct}$ and the average stress $<\boldsymbol{\sigma}>_{NM}$.
- Calculate the secant stiffness tensor $\mathbf{C}_{hom}^{sct}$ using the (Eq.12).
- Calculate the localisation tensor of the strain in the matrix phase

$$\mathbf{A}_{NM} = \frac{1}{f_{NM}}(\mathbf{C}_{NM}^{sct} - \mathbf{C}_i)^{-1}(\mathbf{C}_{hom}^{sct} - \mathbf{C}_i)$$

- Calculate the deformation in the matrix phase NM.

$$\boldsymbol{\varepsilon}_{NM} = \mathbf{A}_{NM} : \mathbf{E}$$

- Calculate the localisation tensor of the deformation in the inclusion phase.

$$\mathbf{A}_i = \frac{1}{f_i}(\mathbf{C}_i - \mathbf{C}_{NM}^{sct})^{-1}(\mathbf{C}_{hom}^{sct} - \mathbf{C}_{NM}^{sct})$$

- Calculate the deformation in the inclusion phase

$$<\boldsymbol{\varepsilon}>_i = \mathbf{A}_i : \mathbf{E}$$

- Verify the accounting of the deformations in the matrix phase

$$\varepsilon_{NM} = ? < \varepsilon >_{NM}$$

- If yes, no more iterations on this pseudo grain.
- Otherwise, perform a new iteration with

$$< \varepsilon >_{NM} = \varepsilon_{NM}$$

- After convergence, we determine the secant homogeneous stiffness $\mathbf{C}^{sct}_{hom_{G_i}}$ of the pseudo grain with Mori Tanaka model:

$$\mathbf{C}^{sct}_{hom_{G_i}} = \mathbf{C}^{sct}_{NM} + f_i(\mathbf{C}^{sct}_i - \mathbf{C}^{sct}_{NM}) : [\mathbf{I} + f_{NM}\mathbf{S}_{Esh}(\mathbf{C}^{sct}_{NM})^{-1} : (\mathbf{C}^{sct}_i - \mathbf{C}^{sct}_{NM})]^{-1}$$

- Calculate the secant modulus of the RVE and the macroscopic stress.

$$\mathbf{C}^{sct}_{hom} = \sum_{i=1}^{N} f_{Gi}\mathbf{C}^{sct}_{hom_{G_i}}$$

$$\mathbf{\Sigma} = \mathbf{C}^{sct}_{hom} : \mathbf{E}$$

IDENTIFICATION MAZARS LAW

From the experimental test on the concrete specimen, we aim to identify the needed parameters of Mazar's model applied to the new mortar. In our analysis, we suppose that all the aggregates introduced in the mortar to prepare the whole concrete remain elastic in all the compressive loading paths. As detailed in the previous section, the parameters of the Mazars model are A_c^{NM}, B_c^{NM}, ε_D^{NM}. As suggested in this law, these parameters fluctuate from reasonable values as stated in Mazars's model identified in our algorithm as a constraint as:

$$1000 < B_c^{NM} < 2000 \ , \ 1 < A_c^{NM} < 2 \ , \ 10^{-5} < \varepsilon_D^{NM} < 10^{-4}$$

The optimization of these parameters involves utilizing a simplex algorithm implemented in Matlab code. The objective is to minimize the residual error between the numerical stress obtained from the homogenization model and the experimental stress depicted in Fig.5. The residual error is calculated using the following equation:

$$R_{er} = \frac{1}{N}\sum_{i=1}^{N}\left[\sigma^{exp}(\varepsilon(i)) - \Sigma_{11}^{hom}(\varepsilon(i), A_c^{NM}, B_c^{NM}, \varepsilon_D^{NM})\right]^2 \qquad (27)$$

with:

R_{er} : Total error.

σ^{exp} : Experimental stress at loading direction.

Σ_{11}^{hom} : Numerical stress estimated by the homogenization model at loading direction, depending on imposed deformation loading $\varepsilon(i)$ and the model parameters A_c^{NM}, B_c^{NM} and ε_D^{NM}.

N: Number of loading step.

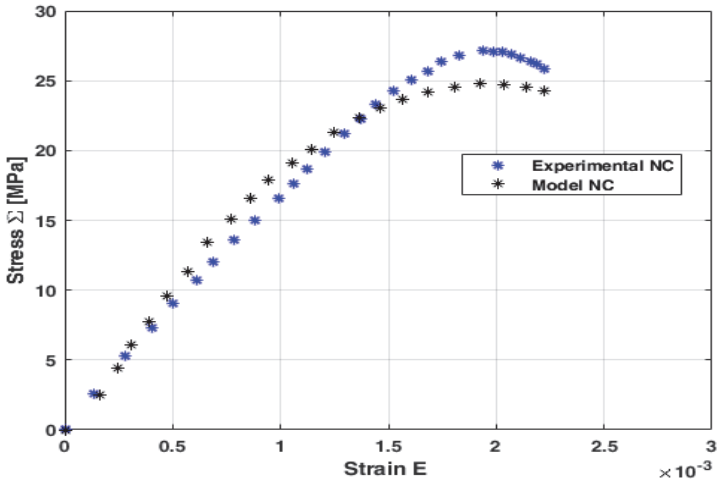

Figure 9: Behavior modelling of natural concrete NC compared to the experimental behavior.

In Fig.9, the experimental stress strain curve of natural concrete NC and the numerical results from the nonlinear homogenization method using the optimized Mazars parameters relative to the new mortar are herein superposed. In this numerical simulation, we assume that the concrete is composed of a single grain composed of new mortar NM and natural aggregate NA. In this case, the natural aggregates remain elastic, and their elastic properties can be taken from the literature [34]. Then, the parameters $A_c^{NM}, B_c^{NM}, \varepsilon_D^{NM}$ obtained by the identification method using the homogenization strategy as described previously are shown in Tab. 4.

Phases	E(GPa)	ν	ε_D^0	A_c	B_c
New mortar	18	0.2	10^{-4}	1.5	400
Natural aggregate	60	0.12	/	6	6

Table 4: Mechanical properties and Mazars parameters of different phases (NM, NA).

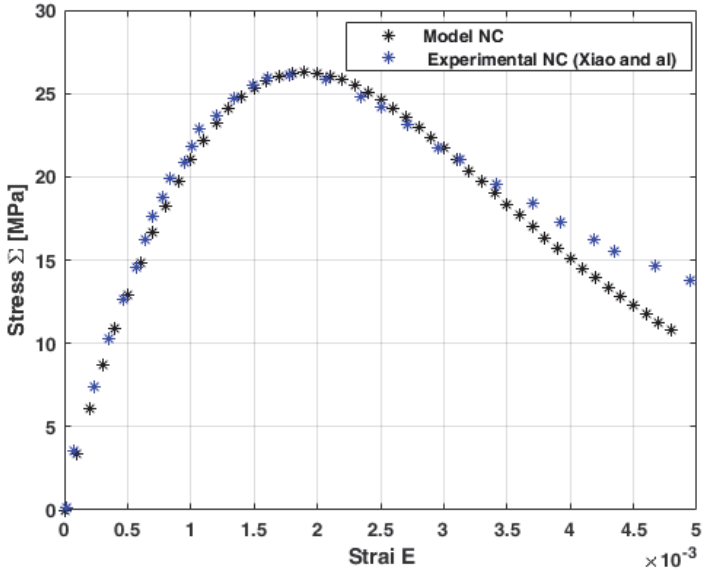

Figure 10: Numerical modelling vs experimental behavior.

Similarly, we apply the identification method to another compressive test of recycled concrete from the work of Xiao [4] in particular the experimental result of natural concrete NC. As mentioned before, new mortar NM obeys to Mazars law [39,40], and the natural aggregate NA remains elastic. Using the identified Mazars's parameters of NM, listed in Tab. 5, the confrontation between the simulation and the experimental results is shown in Fig.10. As we can observe, the identified Mazars's parameters of NM allow us to correctly reproduce the experimental measurements of NC.

Phases	E(GPa)	ν	ε_D^0	A_c	B_c
Mortar	19000	0.18	0.00012	1.1	350
Natural aggregate	60000	0.22	/	/	/

Table 5: Properties of the constituent phases of recycled concrete.

NUMERICAL SIMULATION OF RECYCLED CONCRETE

The multiphase homogenization model proposed in the previous section is used to simulate the compressive tests of different RC specimens and to compare the numerical results with the experimental data. First, we discuss the numerical results in the case of linear elasticity. Secondly, we extend them to nonlinear elasticity. Finally, we confront the proposed model with the experimental results reported in the work of Xiao [4].

Linear properties of recycled concrete

In this first application, all the phases are considered linear, elastic, homogeneous, and isotropic. The shapes of NA and (RAeq) are assumed to be spherical. The mechanical properties of the phases are summarized in Tab. 6, and the elastic properties of old mortar are obtained from literature[34,38]. In the following simulations, the volume fraction of NA is assumed to be 0.4. We start with the calculation of the effective stiffness tensor of the RA using Eq.10. The effective elastic stiffness tensor of the RC is obtained from the mixture law of the equivalent grains calculated by using the Mori-Tanaka model, (Eq.12).

Phases	E(GPa)	ν
New Mortar	60	0.2
Natural aggregate	60	0.08
Old mortar	14	0.3

Table 6: Mechanical properties of RC constituents.

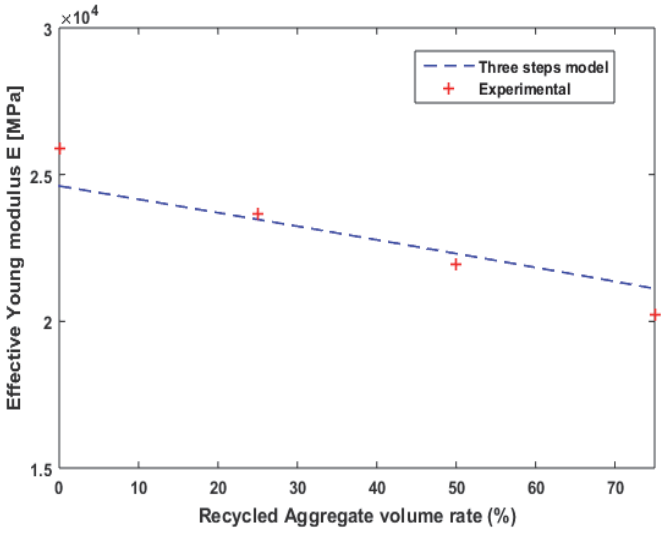

Figure 11: Effective Young modulus of recycled concrete.

Fig.11 presents the effective Young modulus of recycled concrete with respect to recycled aggregate volume rates. The experimental data are also plotted for comparison. One can observe that the maximum difference between the numerical results and the experimental values is less than 5%. Therefore, the proposed homogenization model is highly accurate in predicting the linear elastic behavior of RC. Moreover, the elastic homogenization strategy developed in this study is easy to implement.

Simulation of experimental compressive tests

In this second application, several simulations are carried out to predict the compressive behavior of recycled concrete for varied proportion of RA. Using the identified parameters shown in Tab. 4 and 6, we simulate the compressive behavior of the recycled concretes RC25, RC50 and RC75 considered here as a three-phase composites (NM, NA and RAeq). The nonlinear homogenization strategy described in the previous section is used. We assume that the new mortar matrix obeys to the Mazars law [39,40] and the aggregates remain elastic.

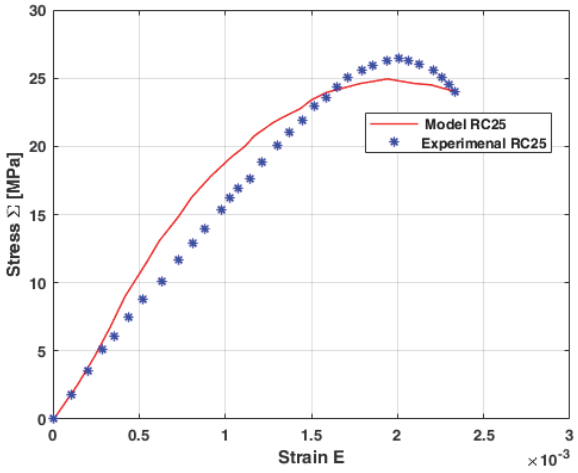

a)- Recycled concrete RC25.

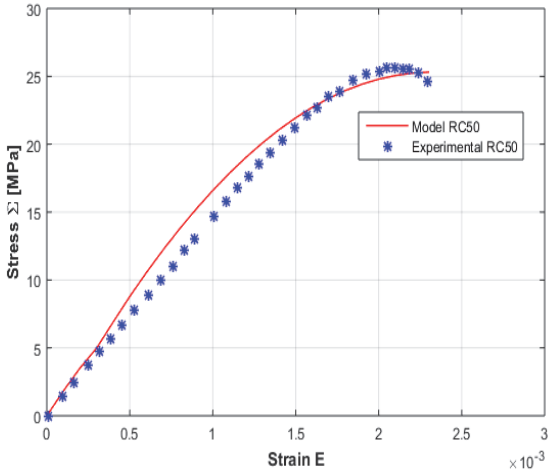

b)- Recycled concrete RC50.

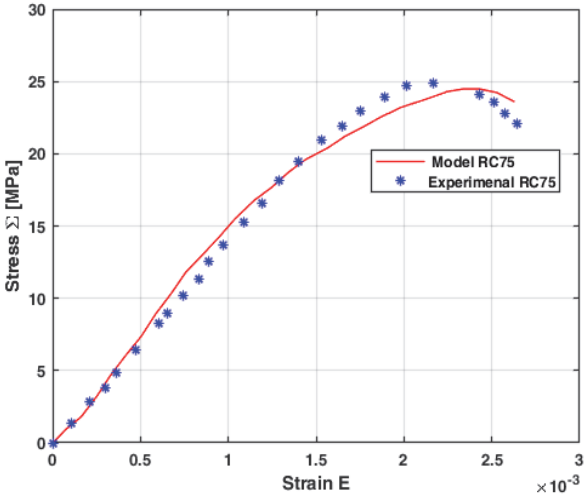

c)- Recycled concrete RC75.

Figure 12: Behaviour modelling of recycled concrete RC compared to the experimental results.

Fig.12.a, 12.b and 12.c show the numerical simulation results compared to the experimental ones. A good agreement was obtained. Tab. 7 shows the experimental and numerical peak stress and its corresponding strain for the different studied recycled concretes. We can notice that the model slightly underestimate the peak stress around 6% of error for RC25. For RC50 and RC75, the difference between the experimental and numerical stress is around 1%. However, the difference between the strain at the peak estimated by the model and that of experimental is generally between 1% to 9%.

Type of concrete	NC	RC25	RC50	RC75
Experimental pic stress	27.13	26.43	25.65	24.84
Numerical pic stress	24.75	24.95	25.31	24.48
Experimental pic strain	0.0019	0.002	0.0021	0.0022
Numerical pic strain	0.001922	0.0019	0.0023	0.0023

Table 7: Numerical and experimental pic stress and strain.

From the results shown in the previous figures and Tab. 7, it can be seen that the numerical model describes well the behavior of concrete. The slope of the numerical stress-strain curve is close to that of the experimental curve, the numerical model estimates correctly the maximum stress. However, the numerical strain at the peak is slightly overestimated compared with the experimental results.

Simulation results with literature Xiao et al [4]

In this last applications, we apply the nonlinear homogenization modelling to simulate the compressive behavior of recycled concretes studied experimentally in [4]. In this work, 5 types of concrete are formulated based on ordinary Portland cement with a compressive strength of 32.5 MPa. The formulation and the physical properties of the natural aggregates and the recycled aggregates are reported in Tabs. 1-2 in [4]. The RA used is from the waste concrete brought from the runway of an airport in Shanghai, PR China.

Tab. 8 presents the experimental and numerical stress and strain peak, from results, the experimental pic stress and strain of NC is 26.07 MPa and 0.0018, respectively, however the values shown by the model are 26.25 MPa and 0.0019, and the model overestimated the pic stress and strain by 0.7% and 5%. For RC100, the experimental pic stress and strain are 23.56MPa and 0.0023, respectively, whereas the numerical model estimates a pic stress and strain of 24.49 MPa and 0.0021, respectively, then the pic stress is underestimated by 3% and the pic strain is overestimated by 8%. The maximum stress estimated at the peak is well predicted, as well as the ultimate strain, in the post peak phase, even if the stress decreases the strain increases, and thus the model predicts almost in perfect agreement.

Type of concrete	NC	RC30	RC50	RC70	RC100
Experimental pic stress	26.07	25.67	24.04	23.49	23.56
Numerical pic stress	26.25	25.32	24.74	24.19	24.49
Experimental pic strain	0.0018	0.0016	0.0019	0.002	0.0023
Numerical pic strain	0.0019	0.002	0.002	0.0023	0.0021

Table 8: Numerical and experimental pic stress and strain.

Fig.13.a, 13.b, 13.c and 13.d show the numerical simulations of the compressive behavior of different RC (RC30, RC50, RC70 and RC100) obtained by the nonlinear secant homogenization model, compared to the experimental data [4]. In the linear phase, the numerical slope is nearly identical to that obtained experimentally. The proposed nonlinear homogenization model allows to correctly estimate the behavior in compression especially before the peak whatever the fraction of recycled aggregates in the concrete. In addition, the maximum stresses of the different concretes are correctly predicted. It can be seen that even though the nonlinear homogenization model reproduces globally correct softening behavior after the peak, a non-negligible overestimation can be observed. This overestimation decreases when the fraction of recycled aggregates increases. These encouraging results concern the results obtained by an approximation of the local fields by their average that is considering a classical secant linearization which tends to overestimate the nonlinear behavior compared to a modified secant linearization [42] and [43]. As already presented previously, this approximation link the stress field linearized by the quadratic mean to the local strain field, for the construction of the nonlinear secant homogenization model. Other ways for improvement can also be envisaged, namely the consideration of a damage law with the consideration of the concrete lateral damage. The difficulty lies in particular in the step of identifying the model parameters, which is an essential step for its prediction efficiency.

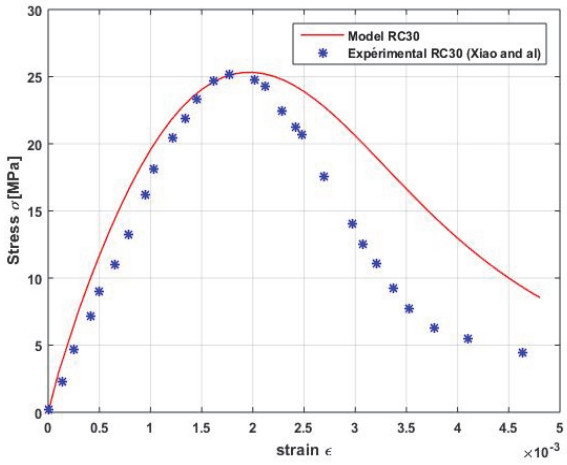

a)- Recycled concrete RC30 .

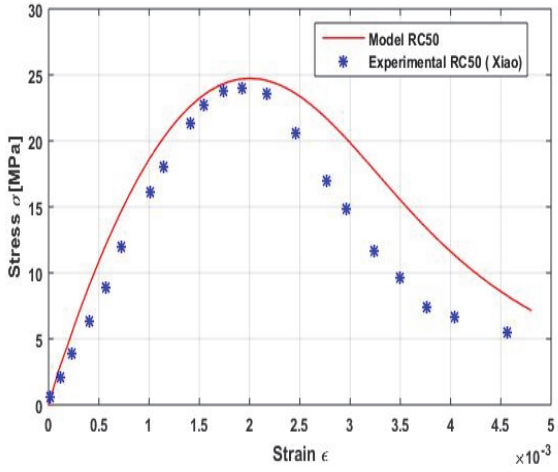

b)- recycled concrete RC50

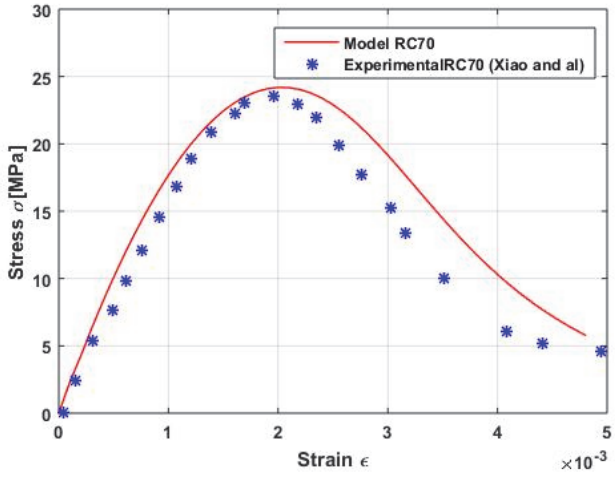

c)- Recycled concrete RC70 .

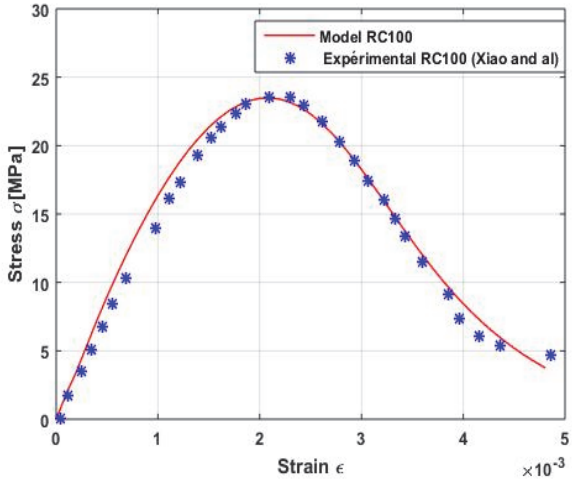

d)- recycled concrete RC100.

Figure 13: Results of numerical modelling for different fraction of recycled aggregates.

Conclusion

This paper presents an experimental and numerical study on recycled concrete. The following remarks and conclusions can be drawn from this work:

1. The experimental work involved uniaxial compression tests on natural concrete (NC) and recycled concrete (RC) with different substitution rates of natural aggregates (NA) by recycled aggregates (RA). The stress-strain curves obtained from these tests showed that the addition of recycled aggregates in the concrete affects its mechanical properties in both the fresh and hardened states. Specifically, the incorporation of recycled aggregates in new concrete leads to a decrease of the Young modulus and the compressive strength, and an increase of the maximal strain.

2. A linear elastic homogenization model for recycled concrete is established by combining the GEEE-MT-Voigt methods through a three-step homogenization procedure. This model is then extended to the nonlinear regime by using a secant formulation. Mazars damage law is incorporated into the model to describe the softening behavior. The recycled concrete can be simulated as a three-phase composite by using the proposed homogenization procedure.

3. The proposed homogenization model was validated by comparing the numerical results with the experimental behavior of NC and different RCs. The numerical predictions show a good agreement with the experimental results for different substitution rates.

Overall, the findings of this study provide valuable insights into the properties and behavior of recycled concrete, and may contribute to the development of more effective methods for incorporating recycled materials into concrete structures.

Acknowledgments

The authors would like to thank the L2MGC laboratory of UMMTO and the LSPM laboratory of the Sorbonne Paris North university, and the Tassili project (PHC – 43940NJ) for their contribution to the realization of this work.

Declaration of interest statement

On behalf of all authors, the corresponding author states that there is no conflict of interest.

References

[1] Manzi, S., Mazzotti, C., Bignozzi, M.C. (2017). Self-compacting concrete with recycled concrete aggregate: Study of the long-term properties, Constr. Build. Mater., 157(2017), pp. 582–590, DOI: 10.1016/j.conbuildmat.2017.09.129.

[2] Yanya, Y. (2018). Blending ratio of recycled aggregate on the performance of pervious concrete, Frat. Ed Integrita Strutt., 12(46), pp. 343–351, DOI: 10.3221/IGF-ESIS.46.31.

[3] Younis, A., Ebead, U., Judd, S. (2018). Life cycle cost analysis of structural concrete using seawater, recycled concrete aggregate, and GFRP reinforcement, Constr. Build. Mater., 175, pp. 152–160, DOI: 10.1016/j.conbuildmat.2018.04.183.

[4] Xiao, J., Li, J., Zhang, C. (2005). Mechanical properties of recycled aggregate concrete under uniaxial loading, Cem. Concr. Res., 35(6), pp. 1187–1194, DOI: 10.1016/j.cemconres.2004.09.020.

[5] Yang, H., Fang, J., Jiang, J., Li, M., Mei, J. (2023). Compressive stress–strain curve of recycled concrete under repeated loading, Constr. Build. Mater., 387(April), pp. 131598, DOI: 10.1016/j.conbuildmat.2023.131598.

[6] Zhou, C., Chen, Z. (2017). Mechanical properties of recycled concrete made with different types of coarse aggregate, Constr. Build. Mater., 134, pp. 497–506, DOI: 10.1016/j.conbuildmat.2016.12.163.

[7] Bhikshma, V. and Kishore, R. (2010). Development of stress-strain curves for recycled aggregate concrete, Asian J. Civ. Eng. (Bulding Housing), 11(2), pp. 253–261.

[8] Xiao, J., Li, W., Sun, Z., Lange, D.A., Shah, S.P. (2013). Properties of interfacial transition zones in recycled aggregate concrete tested by nanoindentation, Cem. Concr. Compos., 37(1), pp. 276–292, DOI: 10.1016/j.cemconcomp.2013.01.006.

[9] Silva, M.P., Mota, M.T., Gadéa, A.S.M., Leite, M.B. , Nagahama, K.J. (2015). The Behavior of Recycled Concrete through the Application of an Isotropic Damage Model, Open J. Civ. Eng., (5), pp. 339–351, DOI: 10.4236/ojce.2015.53034.

[10] Peng, Y., Zakaria, S., Sun, Y., Chen, Y., Zhang, L. (2022). Analysis of tensile strength and failure mechanism based on parallel homogenization model for recycled concrete, Materials (Basel)., 15, pp. 145, DOI: 10.3390/ma15010145.

[11] Gupta, M., Sharma, M., Shashank Bishnoi. (2022). Multiscale modelling of uniaxial compressive stress-strain behaviour of concrete using analytical homogenisation and damage mechanics, Mech. Mater., 173, pp. 104430, DOI: 10.1016/j.mechmat.2022.104430.

[12] Königsberger, M., and., Stéphanie, S. (2018). Micromechanical multiscale modeling of ITZ-driven failure of recycled concrete: Effects of composition and maturity on the material strength, Appl. Sci., 8(6), pp. 1–25, DOI: 10.3390/app8060976.

[13] Sharma, M., Bishnoi, S. (2020). Influence of properties of interfacial transition zone on elastic modulus of concrete : Evidence from micromechanical modelling, Constr. Build. Mater., 246, pp. 118381, DOI: 10.1016/j.conbuildmat.2020.118381.

[14] Bishnoi, S., Scrivener, K.L. (2009). Cement and Concrete Research μic : A new platform for modelling the hydration of

cements, Cem. Concr. Res., 39(4), pp. 266–74, DOI: 10.1016/j.cemconres.2008.12.002.
[15] Pedro, D., Brito, J. De., Evangelista, L. (2017). Mechanical characterization of high performance concrete prepared with recycled aggregates and silica fume from precast industry, J. Clean. Prod., 164, pp. 939–949, DOI: 10.1016/j.jclepro.2017.06.249.
[16] Guo, M., Grondin, F., Loukili, A. (2019). Numerical method to model the creep of recycled aggregate concrete by considering the old attached mortar, Cem. Concr. Res., 118(February), pp. 14–24, DOI: 10.1016/j.cemconres.2019.01.008.
[17] Omary, S., Ghorbel, E., Wardeh, G. (2016). Relationships between recycled concrete aggregates characteristics and recycled aggregates concretes properties, Constr. Build. Mater., 108, pp. 163–174, DOI: 10.1016/j.conbuildmat.2016.01.042.
[18] Pierard, O., Friebel, C., Doghri, I. (2004). Mean-field homogenization of multi-phase thermo-elastic composites : a general framework and its validation, Compos. Sci. Technol., 64(January), pp. 1587–603, DOI: 10.1016/j.compscitech.2003.11.009.
[19] Belin, P., Habert, G., Thiery, M., Roussel, N. (2014). Cement paste content and water absorption of recycled concrete coarse aggregates, Mater. Struct. Constr., 47(9), pp. 1451–65, DOI: 10.1617/s11527-013-0128-z.
[20] Shen, D., Du, J. (2004). Evaluation of building materials recycling on HMA permanent deformation, 18(43), pp. 391–397, DOI: 10.1016/j.conbuildmat.2004.03.007.
[21] Zheng, C., Lou, C., Du, G., Li, X., Liu, Z., Li, L. (2018). Mechanical properties of recycled concrete with demolished waste concrete aggregate and clay brick aggregate, Results Phys., 9(April), pp. 1317–1322, DOI: 10.1016/j.rinp.2018.04.061.
[22] Yousfi, S., Nouri, L., Saidani, M., Hadjab, H. (2014). The use of the dreux-gorisse method in the preparation of concrete mixes: An automatic approach, Asian J. Civ. Eng., 15(1), pp. 79–94.
[23] Caroline, S. R., Mayara, A. Marco, P., Yiming, Y. (2017). Tension stiffening approach for interface characterization in recycled aggregate concrete, Cem. Concr. Compos., 82, pp. 176–189, DOI: 10.1016/j.cemconcomp.2017.06.009.
[24] Puthussery, J. V., Kumar, R., Garg, A. (2017). Evaluation of recycled concrete aggregates for their suitability in construction activities : An experimental study, Waste Manag., 60, pp. 270–276, DOI: 10.1016/j.wasman.2016.06.008.
[25] Mora, J.M. (2015). Effect of mixed recycled aggregates on mechanical properties of recycled concrete, DOI: 10.1680/macr.14.00217.
[26] Andreu, G. and Miren, E. (2014). Experimental analysis of properties of high performance recycled aggregate concrete, Constr. Build. Mater., 52, pp. 227–235, DOI: 10.1016/j.conbuildmat.2013.11.054.
[27] Kwan, W.H., Ramli, M., Kam, K.J., Sulieman, M.Z. (2012). Influence of the amount of recycled coarse aggregate in concrete design and durability properties, Constr. Build. Mater., 26(1), pp. 565–573, DOI: 10.1016/j.conbuildmat.2011.06.059.
[28] Kebaili, B., Benzerara, M., Menadi, S., Kouider, N., Belouettar, R. (2022). Effect of parent concrete strength on recycled concrete performance, Frat. Ed Integrita Strutt., 16(62), pp. 14–25, DOI: 10.3221/IGF-ESIS.62.02.
[29] Pedro, D., De Brito, J., Evangelista, L. (2014). Influence of the use of recycled concrete aggregates from different sources on structural concrete, Constr. Build. Mater., 71, pp. 141–151, DOI: 10.1016/j.conbuildmat.2014.08.030.
[30] Ouaar, A., Doghri, I., Delannay, L., Thimus, J.F. (2007). Micromechanics of the Deformation and Damage of Steel Fiber-reinforced Concrete, Int. J. Damage Mech., 16(2), pp. 227--260, DOI: 10.1177/1056789506064946.
[31] Bombay, P., Bombay, P. (1993). Behaviour of concrete with different proportions of natural and recycled aggregates, 9, pp. 109–126.
[32] Marinkovic, B., Tošic, N., Ignjatovic, I.S. (2017). Shear behaviour of recycled aggregate concrete beams with and without shear reinforcement, 141, pp. 386–401, DOI: 10.1016/j.engstruct.2017.03.026.
[33] Fellah, D., Barboura, S., Tilmatine T., Li J. Kachi M.S., Bouafia, Y. (2021). Studies on elastic properties of recycled concrete by micromechanical modeling, Adv. Mater. Mech. Manuf. II, , pp. 416–434, DOI: 10.1007/978-3-030-84958-0_44.
[34] Adessina, A., Ben, A., Barthélémy, J., Chateau, C., Garnier, D. (2019). Research Experimental and micromechanical investigation on the mechanical and durability properties of recycled aggregates concrete, Cem. Concr. Res., 126(September), pp. 105900, DOI: 10.1016/j.cemconres.2019.105900.
[35] Barboura, S., Li, J., Franciosi, P. (2023). A simple analytical estimate for the elastic-plastic behavior of two-phase bi-continuous isotropic composites, Mech. Adv. Mater. Struct., DOI: https://doi.org/10.1080/15376494.2023.2211407.
[36] Berveiller, M., Zaoui, A. (1978). An extension of the self-consistent scheme to plastically-flowing polycrystals, J. Mech. Phys. Solids, 26(5–6), pp. 325–344, DOI: 10.1016/0022-5096(78)90003-0.
[37] Ghazavizadeh, A., Haboussi, M., Abdul-latif, A., Jafari, A. (2019). A general and explicit Eshelby-type estimator for

evaluating the equivalent stiffness of multiply coated ellipsoidal heterogeneities, Int. J. Solids Struct., 171, pp. 103–116, DOI: 10.1016/j.ijsolstr.2019.04.023.

[38] Rodrigues, E.A., Gimenes, M., Bitencourt, L.A.G., Manzoli, O.L. (2021). A concurrent multiscale approach for modeling recycled aggregate concrete, Constr. Build. Mater., 267, pp. 121040, DOI: 10.1016/j.conbuildmat.2020.121040.

[39] Mazars J. (1986). A description of micro-and macroscale damage of concrete structures. Engineering Fracture Mechanics, 25(5-6), pp. 729-737. DOI: 10.1016/0013-7944(86)90036-6.

[40] Mazars J., Hamon F., Grange S. (2015). A new 3D damage model for concrete under monotonic, cyclic and dynamic loadings. Materials and Structures, 48(11), pp. 3779-3793. DOI: 10.1617/s11527-014-0439-8.

[41] Benyahi, K., Bouafia, Y., Kachi, MS., Hamri, A., Benakli, S. (2021). Periodic homogenization and damage evolution in RVE composite material with inclusion, Frat. Ed Integrita Strutt., 15(58), pp. 319–343, DOI: 10.3221/IGF-ESIS.58.24.

[42] Suquet, P. (1997). Effective properties of nonlinear composites, Contin. Micromecanics, pp. 198–264, DOI: 10.1007/978-3-7091-2662-2_4.

[43] Suquet, P. (1995). Overalle properties of nonlinear composites, Solid Mech. Its Appl., 46, pp. 149–156, DOI: 10.1007/978-94-009-1756-9_19.